Interplay between weak localization of exciton-polaritons and the optical spin Hall effect

T. C. H. Liew,[1] C. Leyder,[3] A. V. Kavokin,[2,4] A. Amo,[3] J. Lefrère,[3] E. Giacobino,[3] and A. Bramati[3]
[1]*Centre for Quantum Technologies, National University of Singapore, Singapore 117543*
[2]*School of Physics and Astronomy, University of Southampton, Highfield, Southampton SO17 1BJ, United Kingdom*
[3]*Laboratoire Kastler Brossel, Université Paris 6, Ecole Normale Supérieure et CNRS, UPMC Case 74, 4 Place Jussieu, 75252 Paris Cedex 05, France*
[4]*Marie-Curie Chair of Excellence "Polariton Devices," University of Rome II, 1, via della Ricerca Scientifica, Rome 00133, Italy*
(Received 27 October 2008; revised manuscript received 2 December 2008; published 16 March 2009)

The multiple scattering of exciton-polaritons by a static disorder in planar microcavities results in their weak localization, characterized by a pronounced backscattering signal. This effect is associated with an enhanced optical spin Hall effect leading to the appearance of ballistic spin currents in the plane of the cavity. We demonstrate experimentally and theoretically the coexistence of these two mesoscopic effects and interplay between them.

DOI: 10.1103/PhysRevB.79.125314 PACS number(s): 71.36.+c, 03.75.Kk, 42.65.−k

I. INTRODUCTION

Exciton-polaritons are electrically neutral quasiparticles that can be optically excited in various solid-state systems,[1] including semiconductor microcavities.[2] Recently, semiconductor microcavities have demonstrated great potential for both fundamental science, with the observation of polariton Bose-Einstein condensation,[3–5] and practical applications, with the promise of polariton lasing.[6–8] These phenomena are the upshot of the light effective mass and relatively large coherence length of polaritons. Such polariton properties also give rise to other various mesoscopic effects including weak localization[9] and resonant backscattering.[10,11] These related effects are general properties of disordered systems[12] in which waves can become trapped in potential minima or undergo elastic scattering.

Other applications of semiconductor microcavities rely on the fact that polaritons carry spin.[13] The potential of microcavities for spintronic devices was recently raised with the experimental observation of the optical spin Hall effect (OSHE),[14] which consists of the optical generation and manipulation of polariton spin currents in a microcavity plane. The OSHE implies the resonant Rayleigh scattering of polaritons; that is, since the energy of polaritons depends only on their absolute wave vector (apart from a minor influence of longitudinal-transverse splitting), polaritons can elastically scatter to any point on a circle in reciprocal space [see Fig. 1(a)]. The ballistic propagation of scattered polaritons is accompanied by precession of their pseudospins (or Stoke's vectors[15]) around an effective magnetic field proportional to the splitting between transverse electric and transverse magnetic polariton modes. This rotation results in the buildup of right- or left-circular polarization (depending on the direction of scattering) and leads to the formation of polariton spin currents. The coherence of the polariton system is maintained by the OSHE.

Although the potential experienced by polaritons in microcavities is continuous, the physics is qualitatively identical to the scattering of waves in a discrete random medium in which the positions of scattering points are fixed. The interference of different scattering paths determines the exact angular distribution of scattered polaritons, which tends to result in a fast-varying function of the scattering angle. This gives rise to the well-known speckle pattern. Smooth correlations of the disorder potential privilege the scattering at small angles. The multiple scattering leads to the enhancement of backscattering; any multiple-scattering path carries exactly the same phase change as the reverse path, which allows constructive interference if the input and output wave vectors are oppositely oriented [Fig. 1(c)]. This well-known mesoscopic effect has been observed for polaritons.[11]

There is an interplay between the OSHE and the resonant backscattering/weak localization, which we demonstrate experimentally in this paper by polarization, wave vector and spatially resolved measurements of the resonant Rayleigh scattering from a microcavity. For backscattering to occur in a given area in a microcavity sample, the polariton lifetime, τ, must be sufficiently larger than the mean time between scattering events, τ_s, to allow multiple-scattering paths to interfere. Hence the appearance of a backscattering peak represents an area on the sample with relatively long polariton lifetime. In such areas we can thus expect the long-distance propagation of polariton spin currents. Theoretically, the effects of disorder are described by a Schrödinger equation for the spinor polariton wave function.

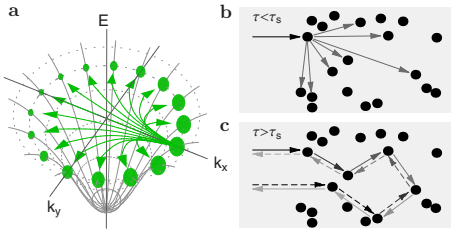

FIG. 1. (Color online) (a) The polariton dispersion: polaritons created at a given wave vector (e.g., along k_x) can elastically scatter to any point around a circle in reciprocal space. (b) The first-order scattering of polaritons dominates the secondary emission of the cavity when the mean time between scattering events, τ_s, is greater than the polariton lifetime, τ. (c) When $\tau > \tau_s$ multiple polariton scattering is significant and constructive interference between reverse paths (shown by solid and dotted arrows) enhances backscattering.

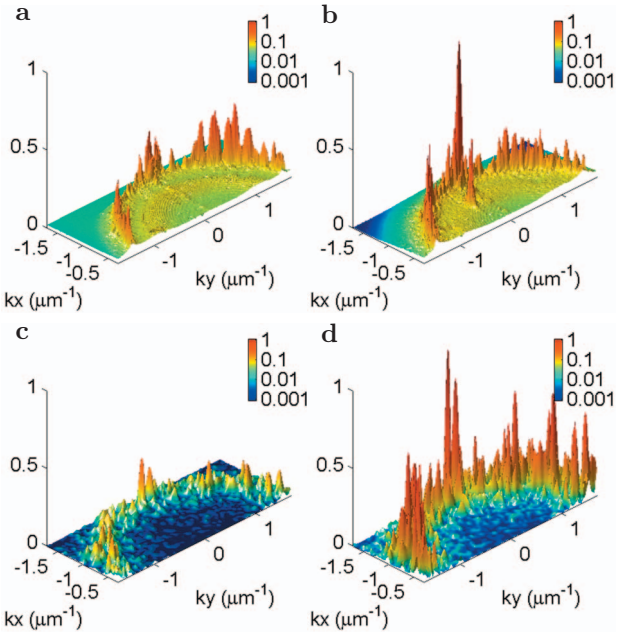

FIG. 2. (Color) Three-dimensional plots showing the time integrated intensity in the region in the far field where backscattering is expected. The vertical scale is a linear scale in intensity; the colors represent a logarithmic scale. Panels (a) and (b) show the results measured from points A and B on the sample, respectively. (c) and (d) show the results from theoretical modeling with polariton lifetimes equal to 5 and 10 ps, respectively.

II. EXPERIMENT

The sample and the experimental setup we used is described in Refs. 16 and 14, respectively. We studied a high-quality factor 2λ GaAs/AlAs cavity with three low indium content $In_{0.04}Ga_{0.96}As$ quantum wells—one at each antinode of the cavity mode. The Rabi splitting energy is 5.1 meV. Polariton linewidths are in the 100 μeV range, corresponding to a lifetime τ in the 1–10 ps range. We excited the sample at an angle of 12° with linearly polarized light (the polarization was checked to a precision of 2% using a polarizing beam splitter and photodetector). The pump is focused on the microcavity to a spot of 50 μm diameter. The microcavity is cooled at 4 K in a cold finger cryostat. The transmitted intensity is collected, polarization resolved, and imaged on 1024×1024 charge-coupled device cameras. The imaging is done in the near and far field using a 50 mm lens. The detected intensities in the two circular polarizations, I_+ and I_-, give the circular polarization degree, $\rho_c=(I_+-I_-)/(I_++I_-)$, in both near and far fields.

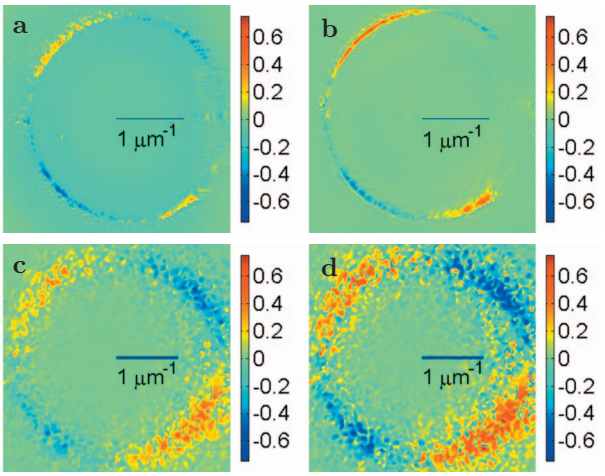

FIG. 3. (Color) The circular polarization degree in the far field. Panels (a)–(d) correspond to the same situations in Figs. 2(a)–2(d).

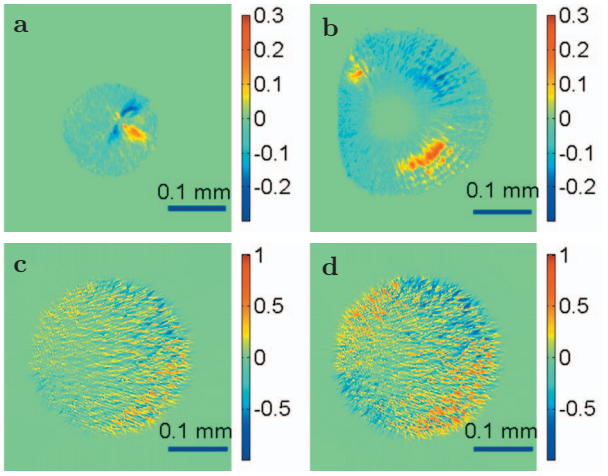

FIG. 4. (Color) The circular polarization degree in the near field. (a) and (b) show the results measured from points A and B on the sample, respectively. (c) and (d) show the results from theoretical modeling with polariton lifetimes equal to 5 and 10 ps, respectively.

Let us first discuss measurements from two points on the microcavity sample, A and B. In Figs. 2–4 the results are compared with a theoretical model (presented in Sec. III). At point A there is no significant backscattering signal [Fig. 2(a)]. In this regime we see only weak short propagating spin currents appearing from the OSHE [Fig. 4(a)]. At point B there is a large backscattering signal [Fig. 2(b)] and we observe strong long propagating spin currents [Fig. 4(b)] propagating over distances of the order of 100 μm. The exciton-photon detuning is −0.5 meV at point A and −0.3 meV at point B, which results in a shorter polariton lifetime at point A than at point B. This difference is apparently enhanced by the photonic disorder. From Fig. 4(a) we make an order-of-

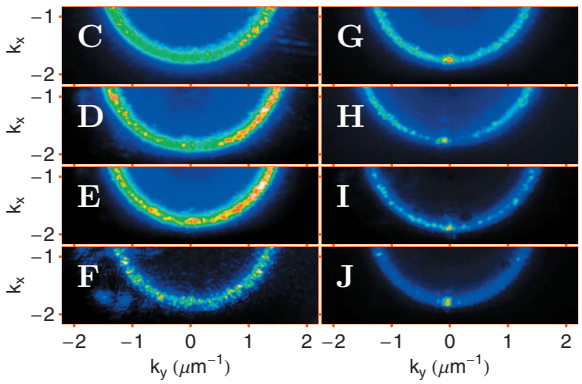

FIG. 5. (Color) Far-field intensity for a selection of different points, labeled C-J, across the sample.

magnitude estimate of the mean-free-path length as 10 μm. Given that the group velocity of polaritons is about 1.3×10^6 m/s this gives a scattering time of $\tau_s \approx 7.5$ ps. Since the polariton lifetime has a similar order of magnitude, we expect that changes in the polariton lifetime can cause transitions between the single-scattering and multiple-scattering regimes.

III. THEORY

Due to their long decoherence time,[17] it is often a reasonable approximation to describe polaritons by a wave function rather than a density matrix. Such an approximation has been used to study superfluid effects of polaritons,[18–21] the effect of energy shifts on parametric oscillators,[22–25] and the description of polariton interference.[26] In this approximation we describe polaritons by a wave function, $\psi_i(\mathbf{k})$, where the index i represents either spin-up (+) or spin-down (−) polaritons.[27] We will consider only lower branch polaritons since for our experimental conditions there is no mechanism to excite upper branch polaritons. Working in reciprocal space, the two-dimensional wave function obeys a Schrödinger equation (in the linear regime) with a random potential representing the disorder in the system,

$$i\hbar \frac{\partial \psi_i(\mathbf{k})}{\partial t} = \hat{\mathbf{H}}_{ij}(\mathbf{k})\psi_j(\mathbf{k}) + \int V(\mathbf{k}')\psi_i(\mathbf{k}-\mathbf{k}')d\mathbf{k}' + f_i(\mathbf{k}) - \frac{i\hbar}{2\tau}\psi_i(\mathbf{k}). \quad (1)$$

The Hamiltonian can be written as

$$\hat{\mathbf{H}}_{ij}(\mathbf{k}) = \delta_{ij}T(\mathbf{k}) + \frac{\hbar}{2}[\sigma \cdot \Omega(\mathbf{k})]_{ij}, \quad (2)$$

where $T(\mathbf{k})$ represents the nonparabolic dispersion of lower branch polaritons, σ is the Pauli-matrix vector, and $\mathbf{\Omega}$ is an effective magnetic field, which is governed by the longitudinal-transverse (LT) splitting of polaritons.[15] The LT splitting causes mixing between the different spin components and provides a mechanism for spin symmetry breaking. In other excitation schemes the LT splitting can lead to unique polarization[17,19] and phase/vortex[28] patterns. For our excitation scheme, where we generate an elastic circle in reciprocal space (using Rayleigh scattering), the LT splitting causes different circular polarizations to emerge in the four quadrants (as seen in Fig. 3). This is the OSHE and the reason for such a pattern can be related to the unique directional dependence of the effective magnetic field.[14,15]

Disorder is represented by two potential fields in real space, $V_C(\mathbf{r})$ and $V_X(\mathbf{r})$, corresponding to the disorder experienced by photons and excitons, respectively. Each field is a stochastic field characterized by root-mean-square amplitudes, $A_{C,X}$, and Gaussian correlation lengths, $\sigma_{C,X}$. The procedure for generating such potentials was the same as in Ref. 12; a collection of Gaussian functions at different points in space is superimposed with random weights. $V(\mathbf{k})$ is the sum of the Fourier transforms of $V_C(\mathbf{r})$ and $V_X(\mathbf{r})$, weighted by the Hopfield factors[29,30] for photons and excitons. Note that this form of the potential is an approximation; in reality the disorder can be anisotropic, which can further enhance the number of backscattered polaritons.[16]

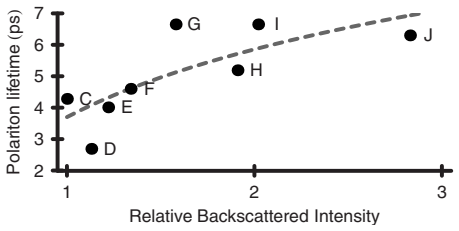

FIG. 6. The polariton lifetime and intensity of the backscattering signal for points C-J. The intensity is measured relative to the background Rayleigh intensity, such that an intensity of 1 corresponds to no enhanced backscattering.

The continuous-wave optical pump is represented by

$$f_i(\mathbf{k}) = A_i e^{-(\mathbf{k}-\mathbf{k}_p)^2 L^2/4} \frac{i\Gamma e^{-iE_p t/\hbar}}{T(\mathbf{k}) - E_p - i\Gamma}. \quad (3)$$

This represents the introduction of polaritons in the system by a Gaussian shaped pump with wave vector $\mathbf{k}_p$, energy E_p, linewidth Γ, spot size L, and amplitude and polarization given by A_i. We choose $(A_+, A_-) = (1, 1)$ for an x-linearly polarized pump and $(A_+, A_-) = (i, -i)$ for a y-linearly polarized pump. The decay of polaritons caused by exciton recombination and the escape of photons through the Bragg mirrors of the microcavity is modeled phenomenologically with a lifetime, τ. Since in the experiment under consideration all polaritons have a similar magnitude of in-plane wave vector any variation in τ with the in-plane wave vector (caused by varying photonic fraction) is neglected. Setting the initial polariton fields to zero, Eq. (1) can be solved numerically using a time propagation method to yield the evolution in reciprocal space. The polariton fields are easily obtained in real space using an inverse Fourier transform. The fields become stationary within 30 ps.

The results of our calculations are shown in Figs. 2–4 for two different polariton lifetimes, 5 and 10 ps, representing different points on the sample. Given the scattering time of $\tau_s \approx 7.5$ ps, these two points correspond, respectively, to the regimes in which single scattering [Fig. 1(b)] and multiple scattering [Fig. 1(c)] are dominant. The parameters used were $k_p = 1560$ mm^{-1}, $\Gamma = 0.2$ meV, $L = 42$ μm (corresponding to full width at half maximum of 50 μm), $A_C = 0.4$ meV, $A_X = 0.15$ meV, $\sigma_C = 1$ μm, and $\sigma_X = 0.3$ μm. The LT splitting was 0.05 meV at the pump wave vector. The polariton dispersion was calculated using a two coupled oscillator model,[30] in which the photon and exciton masses were $3 \times 10^{-5} m_0$ and $0.22 m_0$ respectively, where m_0 is the free-electron mass. The Rabi splitting was 5.1 meV as in the experiment.

IV. DISCUSSION

For short polariton lifetime the backscattering is weak [Fig. 2(c)] and only weak polariton spin currents appear [Fig. 4(c)]. This situation corresponds to the experimental results from point A on the sample [Figs. 2(a) and 4(a)]. For long

lifetime the propagation of spin currents over distances of the order of 100 μm [Fig. 4(d)] is associated with a backscattering peak [Fig. 2(d)]. This situation corresponds to the experimental results from point B on the sample [Figs. 2(b) and 4(b)]. Clearly, a longer lifetime is favorable both for the OSHE and resonant backscattering. Both effects coexist if $\tau > \tau_s$. We note that some differences appear between experiment and theory, particularly in the real-space images of Fig. 4 and we attribute these to our approximation of the structure of disorder, which takes a very specific form in reality. In our study we have understood that Fig. 4(a) can be more closely reproduced theoretically by the introduction of an additional single point defect; however in this paper we wish to concentrate on the relationship between the polariton lifetime and the backscattering. For this reason we do not introduce changes in the disorder structure into our theory; however we respect that changes in the disorder structure are almost certainly present in the experiment.

We also performed measurements on other points across the sample (Fig. 5). A correlation between the backscattered intensity and the lifetime measured at each point (Fig. 6) confirms our interpretation that backscattering is associated with longer polariton lifetimes.

Theoretically, the circular polarization degree of spin currents [Figs. 4(c) and 4(d)] can lie anywhere within the range of $-1-+1$. However, experimentally the measured circular polarization degree of spin currents [Figs. 4(a) and 4(b)] is less, obtaining values between -0.3 and 0.3. This difference can be expected from the fact that the polariton distribution is not fully coherent, particularly due to phonon-polariton scattering, which is not accounted for. The polarization conversion efficiency, including a quantum correction, has been considered in detail recently.[31]

V. CONCLUSION

By allowing the separation of spin currents in real and reciprocal space, the OSHE could be at the heart of future spintronic devices based on semiconductor microcavities. For this reason it is important to understand the conditions under which the OSHE is enhanced and those under which it is suppressed. In this paper we studied the correlation between the enhanced resonant backscattering/weak localization and the OSHE. For some points on a microcavity sample, with weak backscattering, the OSHE is strongly inhibited. However, it is still possible to manufacture OSHE reliant devices by using other points on the sample where the backscattering is strong. Both effects need a relatively long polariton lifetime to be pronounced. They are suppressed with increase of the (negative) exciton-photon detuning, which shortens the polariton lifetime.

Finally we would like to comment on the expected effects of nonlinearity, which could be the subject of future work. In the nonlinear regime, the interaction energy between polaritons raises their energy above the disorder potential. This can reduce the resonant Rayleigh scattering and lead to a superfluid regime.[32,33] Correspondingly we expect the OSHE to be suppressed in regions of high polariton density (near the center of a pump-laser spot). However, it is possible that some scattering centers will still have sufficiently high potential to scatter polaritons, such that polarized spin currents can still be realized via the OSHE. However, the interaction energy of polaritons in these spin currents will overcome the majority of the disorder potential; the spin currents could travel over larger distances than observed in the linear regime, possibly undergoing superfluid propagation.

ACKNOWLEDGMENTS

We thank A. Poddubny, I. A. Shelykh, G. Malpuech, and M. M. Glazov for useful discussions.

[1] V. M. Agranovich, Sov. Phys. Usp. **3**, 427 (1960) [Usp. Fiz. Nauk **71**, 141 (1960)].
[2] A. V. Kavokin and G. Malpuech, *Cavity Polaritons* (Elsevier, New York, 2003).
[3] J. Kasprzak, M. Richard, S. Kundermann, A. Baas, P. Jeambrun, J. M. J. Keeling, F. M. Marchetti, M. H. Szymańska, R. André, J. L. Staehli, V. Savona, P. B. Littlewood, B. Deveaud, and Le Si Dang, Nature (London) **443**, 409 (2006).
[4] R. Balili, V. Hartwell, D. Snoke, L. Pfeiffer, and K. West, Science **316**, 1007 (2007).
[5] C. W. Lai, N. Y. Kim, S. Utsunomiya, G. Roumpos, H. Deng, M. D. Fraser, T. Byrnes, P. Recher, N. Kumada, T. Fujisawa, and Y. Yamamoto, Nature (London) **450**, 529 (2007).
[6] A. V. Kavokin, G. Malpuech, and F. Laussy, Phys. Lett. A **306**, 187 (2003).
[7] S. Christopoulos, G. Baldassarri Höger von Högersthal, A. Grundy, P. G. Lagoudakis, A. V. Kavokin, J. J. Baumberg, G. Christmann, R. Butté, E. Feltin, J. F. Carlin, and N. Grandjean, Phys. Rev. Lett. **98**, 126405 (2007).
[8] D. Bajoni, P. Senellart, E. Wertz, I. Sagnes, A. Miard, A. Lemaître, and J. Bloch, Phys. Rev. Lett. **100**, 047401 (2008).
[9] M. Litinskaia, G. C. La Rocca, and V. M. Agranovich, Phys. Rev. B **64**, 165316 (2001).
[10] W. Langbein, E. Runge, V. Savona, and R. Zimmermann, Phys. Rev. Lett. **89**, 157401 (2002).
[11] M. Gurioli, F. Bogani, L. Cavigli, H. Gibbs, G. Khitrova, and D. S. Wiersma, Phys. Rev. Lett. **94**, 183901 (2005).
[12] V. Savona and W. Langbein, Phys. Rev. B **74**, 075311 (2006).
[13] I. A. Shelykh, K. V. Kavokin, A. V. Kavokin, G. Malpuech, P. Bigenwald, H. Deng, G. Weihs, and Y. Yamamoto, Phys. Rev. B **70**, 035320 (2004).
[14] C. Leyder, M. Romanelli, J.-Ph. Karr, E. Giacobino, T. C. H. Liew, M. M. Glazov, A. V. Kavokin, G. Malpuech, and A. Bramati, Nat. Phys. **3**, 628 (2007).
[15] A. V. Kavokin, G. Malpuech, and M. M. Glazov, Phys. Rev. Lett. **95**, 136601 (2005).

[16] R. Houdré, C. Weisbuch, R. P. Stanley, U. Oesterle, and M. Ilegems, Phys. Rev. B **61**, R13333 (2000).
[17] W. Langbein, I. Shelykh, D. Solnyshkov, G. Malpuech, Yu. Rubo, and A. Kavokin, Phys. Rev. B **75**, 075323 (2007).
[18] I. Carusotto and C. Ciuti, Phys. Rev. Lett. **93**, 166401 (2004).
[19] I. A. Shelykh, Yu. G. Rubo, G. Malpuech, D. D. Solnyshkov, and A. Kavokin, Phys. Rev. Lett. **97**, 066402 (2006).
[20] Yu. G. Rubo, A. V. Kavokin, and I. A. Shelykh, Phys. Lett. A **358**, 227 (2006).
[21] I. A. Shelykh, Yu. G. Rubo, and A. V. Kavokin, Superlattices Microstruct. **41**, 313 (2007).
[22] N. A. Gippius, S. G. Tikhodeev, V. D. Kulakovskii, D. N. Krizhanovskii, and A. I. Tartakovskii, Europhys. Lett. **67**, 997 (2004).
[23] D. M. Whittaker, Phys. Rev. B **71**, 115301 (2005).
[24] D. M. Whittaker, Phys. Status Solidi C **2**, 733 (2005).
[25] D. Sanvitto, D. N. Krizhanovskii, D. M. Whittaker, S. Ceccarelli, M. S. Skolnick, and J. S. Roberts, Phys. Rev. B **73**, 241308(R) (2006).
[26] C. Leyder, T. C. H. Liew, A. V. Kavokin, I. A. Shelykh, M. Romanelli, J. Ph. Karr, E. Giacobino, and A. Bramati, Phys. Rev. Lett. **99**, 196402 (2007).
[27] I. A. Shelykh, A. V. Kavokin, and G. Malpuech, Phys. Status Solidi B **242**, 2271 (2005)
[28] T. C. H. Liew, A. V. Kavokin, and I. A. Shelykh, Phys. Rev. B **75**, 241301(R) (2007).
[29] H. Haug and S. W. Koch, *Quantum Theory of the Optical and Electronic Properties of Semiconductors* (World Scientific, Singapore, 1994).
[30] F. P. Laussy, G. Malpuech, A. V. Kavokin, and P. Bigenwald, J. Phys.: Condens. Matter **16**, S3665 (2004).
[31] M. M. Glazov and L. E. Golub, Phys. Rev. B **77**, 165341 (2008).
[32] G. Malpuech, D. D. Solnyshkov, H. Ouerdane, M. M. Glazov, and I. Shelykh, Phys. Rev. Lett. **98**, 206402 (2007).
[33] D. D. Solnyshkov, H. Ouerdane, M. M. Glazov, I. A. Shelykh, and G. Malpuech, Solid State Commun. **144**, 390 (2007).